TIDAL STRESS AND FAILURE IN THE MOON OF BINARY ASTEROIDS: APPLICATION TO DIDYMOS. L. Pou[1,2], N. Murdoch[2], R. F. Garcia[2], D. Mimoun[2], O. Karatekin[3]. [1]Dept. Earth and Planetary Science, University of California Santa Cruz, Santa Cruz, CA 95064, USA. [2]DEOS/SSPA, ISAE-Supaero, Toulouse, France. [3]Royal Observatory of Belgium, Brussels, Belgium.

Summary: We combine calculations of the tidal stresses inside the secondary of binary asteroids with the Mohr Coulomb failure criterion in order to determine where material failure occurs. Application to several internal models of binary asteroid (65803) Didymos shows that failure is the most likely to occur at the poles and at the surface of the secondary [1].

Introduction: Rocky remnants left over from the early formation of the Solar System, asteroids are a target of choice for planetary science missions since much about the history of planetary formation and small body evolution processes can be learnt by studying them. Here we consider the case of the binary asteroid (65803) Didymos, the target of several future missions e.g., HERA [2] and DART [3]. The stability of the binary asteroid system has important consequences for their evolution, and also for the Hera Cubesats [2] that will touch down on the surface of Didymoon. Additionally, tidally generated quakes could be a potential seismic source for a passive seismology experiment.

Tidal stress calculations: Based on the works of [4-7], tidal displacements and stress are calculated by solving the equations of elastic deformation for an auto-gravitating body, starting at the core of the body up to the surface with tidal potential boundary conditions. Those tidal deformations are calculated for 32 points of the orbit over the whole volume of the studied body. The body is assumed to be spherical and tidally locked to the primary.

Failure criterion: The likelihood of material failure is determined by using the Mohr Coulomb criterion. Well-used in terrestrial geology and seismology [8], this criterion assumes that for failure to be reached, the shear stress τ_m must be stronger than both the cohesion of the body c and the normal stress σ_m . The lithostatic pressure is taken into account as normal stress, and angle of friction Φ is accounted as a factor before the normal stress; thus, the shear stress τ_m must be higher than the Mohr Coulomb criterion:

$$C_{mc}(c, \sigma_m, \Phi) = c + \sigma_m \tan \Phi \qquad (1)$$

Modeling of Didymos: Following [9,10], we assume that Didymain (the primary) and Didymoon (the secondary) both have a bulk density of 2146 kg/m3, with an uncertainty of 30%. The mean diameter of Didymain is 775 m, and the mean distance between the center of the primary and the center of the secondary is 1180 m. Didymoon has a mean diameter of 163 m and a likely retrograde orbit around Didymain with a rotation period of 11.9 h. For this study, we take an orbit eccentricity of 0.03, and assume that Didymoon is a cohesionless body.

For the tidal stress calculations, we model Didymoon as a spherical, layered body with different internal structures: a homogeneous model, with the bulk density from [10] and two models with a 1-meter and 10-meter regolith layer on top of a stronger internal core with physical parameters identical to the homogeneous model, as shown in Figure 1. More details on the internal structure models are given in [1].

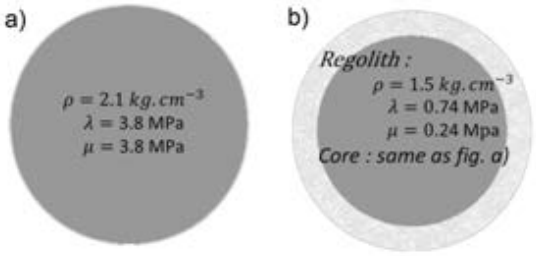

Figure 1. Homogeneous model of Didymos (a, left), and regolith-layered model of Didymos (b, right).

Results: Using the internal structure models of Didymoon presented in Fig. 1, stress maps were calculated. The stresses were diagonalized in order to apply the Mohr Coulomb criterion and find where failure is expected to be reached (Fig. 2). Our calculations show that although the tidal stresses are strongest at the equator, the shear stress is strongest at the poles. Therefore, material failure due to tidal stresses is the most likely to occur at the poles. For a reasonable angle of internal friction (~30°) this failure occurs at the surface down to a few centimeters depth depending on the internal structure model. The homogeneous model reaches failure deeper than the two others (Fig. 3): for the three

models considered, all failure is concentrated in the surface layers. The position on the orbit where the stresses are optimal for failure is at mean anomaly M = π/2, which means halfway between the perigee and the apogee.

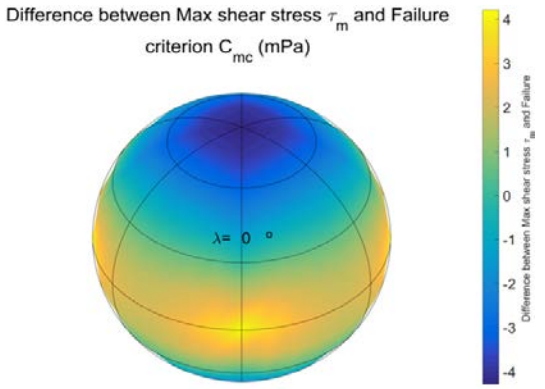

Figure 2. Areas where failure is reached (blue). Plot is made at the surface of the body, with mean anomaly of π/2.

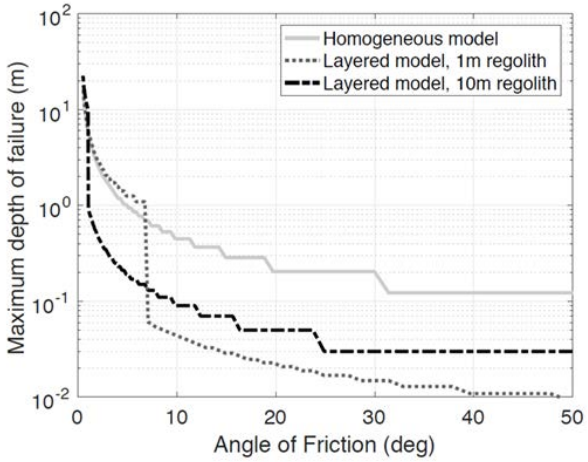

Figure 3. Depth of failure depending of the angle of friction for all three models. Discontinuities are due to the quantifications of the layers into sub-layers for the tidal calculations.

Spheroid corrections: In order to match the true shape of Didymoon better [9], spheroid corrections for the homogeneous model were added using the works from [11], shown in Figure 4. These corrections amplify stresses but especially shear stress. As a consequence, a spheroid body is more likely to reach failure at a given position.

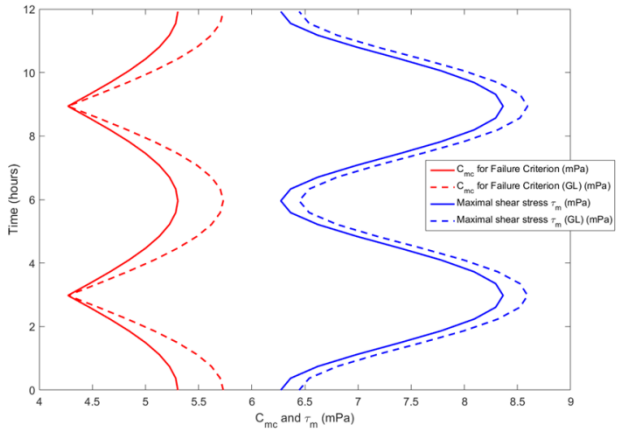

Figure 4. Comparison between shear stress (blue) and Mohr Coulomb criterion (red) for a spherical body (solid line) and a spheroid body (dotted line, GL as reference from [11]). Failure is the most likely to happen when the blue curve is above the red curve.

Conclusion: Material failure due to tidal stress in the secondary of binary asteroids is found to be the most likely at the poles of the body and at its surface, assuming a spherical or spheroid body with no cohesion and either homogeneous or two-layered. These results imply that any linear features, faults or regolith motion observed near the poles of Didymoon could be due to tidal stresses.

Acknowledgements: This study was possible thanks to financial support from the French space agency (CNES), the European space agency (ESA) and the French national agency for research (ANR).

References: [1] Murdoch, N. et al. (2017). *Planetary and Space Science* **144**, 89-105. [2] Michel, P. et al. (2018). *Advances in Space Research* **62**, 2261-2272. [3] Cheng, A. F. et al. (2016). *Planetary and Space Science* **121**, 27-35. [4] Alterman, Z. et al. (1959). *Proceedings of the Royal Society A* **252**, 80-95. [5] Peltier, W. R. and Andrews, J. T. (1976). *Geophysical Journal of the Royal Astronomical Society* **46**, 605-646. [6] Longman, I. M. (1963). *Journal of Geophysical Research* **68**, 485-496. [7] Arkani-Hamed, J. (1973). *The moon* **6**, 100-111. [8] Lay, T. and Wallace, T. C. (1995). *Academic Press, San Diego*. [9] AIM-A Team. (2015). *ESA document reference: AD3-AIMA*. [10] Scheirich, P. and Pravec, P. (2009). *Icarus* **200**, 531-547. [11] Greff-Lefftz, M. et al. (2005). *Celestial Mechanics and Dynamical Astronomy* **93**, 113-146.